Published in final edited form as:
Cell Metab. 2014 October 7; 20(4): 593–602. doi:10.1016/j.cmet.2014.08.012.

Metabolic Inflexibility Impairs Insulin Secretion And Results In MODY-like Diabetes In Triple FoxO-deficient Mice

Ja Young Kim-Muller[1], **Shangang Zhao**[3], **Shekhar Srivastava**[2], **Yves Mugabo**[3], **Hye-Lim Noh**[1], **YoungJung R. Kim**[4], **S.R. Murthy Madiraju**[3], **Anthony W. Ferrante**[1], **Edward Y. Skolnik**[2], **Marc Prentki**[3], and **Domenico Accili**[1]

[1]Naomi Berrie Diabetes Center, Department of Medicine, Molecular and Biomedical Studies Columbia University, New York, NY 10032 USA

[2]Division of Nephrology, The Helen L. and Martin S. Kimmel Center for Biology and Medicine at the Skirball Institute for Biomolecular Medicine, New York University Langone Medical Center, New York, NY 10016 USA

[3]Molecular Nutrition Unit and Montreal Diabetes Research Center at the CRCHUM and Departments of Nutrition and Biochemistry, and Molecular Medicine, Université de Montréal, Montréal, H2X 0A9, Canada

[4]Department of Genetics and Integrated Program in Cellular, Molecular and Biomedical Studies Columbia University, New York, NY 10032 USA

Abstract

Pancreatic β-cell failure in type 2 diabetes is associated with functional abnormalities of insulin secretion and deficits of β-cell mass. It's unclear how one begets the other. We have shown that loss of β-cell mass can be ascribed to impaired FoxO1 function in different models of diabetes. Here we show that ablation of the three FoxO genes (1, 3a, and 4) in mature β-cells results in early-onset, maturity onset diabetes of the young (MODY)-like diabetes, with abnormalities of the MODY networks of Hnf4α, Hnf1α, and Pdx1. FoxO-deficient β-cells are metabolically inflexible, i.e., they preferentially utilize lipids rather than carbohydrates as an energy source. This results in impaired ATP generation, and reduced Ca^{2+}-dependent insulin secretion. The present findings demonstrate a secretory defect caused by impaired FoxO activity that antedates dedifferentiation. We propose that defects in both pancreatic β–cell function and mass arise through FoxO-dependent mechanisms during diabetes progression.

Correspondence: Domenico Accili, MD, 1150 St. Nicholas Ave. New York, NY 10032, Tel. 212-851-5332, FAX 212-851-5335, da230@columbia.edu.

Introduction

Patients with type 2 diabetes display qualitative and quantitative defects in pancreatic β-cell function and mass (Ferrannini, 2010). These deficits are the critical components of the transition from compensated insulin resistance (Weyer et al., 1999)– a state that may affect up to a quarter of the population (Reaven, 1995)– to overt hyperglycemia, a condition that affects 5–8% of the population (National Institute of Diabetes and Digestive and Kidney Diseases, 2005). Functional defects appear to antedate quantitative ones at the onset of hyperglycemia (Prentki and Madiraju, 2012; Rahier et al., 2008), but there is no clear mechanism to explain how β-cell dysfunction spawns loss of β-cells.

The functional impairment of β-cells has both genetic (Fajans and Bell, 2011) and acquired components, with the latter being partly reversible, at least initially (Savage et al., 1979). Thus, a challenge for this field of investigation is to identify mechanisms whereby genetic, environmental, and reversible defects of β-cell function can be subsumed with loss of β-cell mass under a general theory of β-cell failure (Accili et al., 2010).

Transient elevations of glucose or lipids activate transcription factor FoxO1 through nuclear translocation in β-cells (Kawamori et al., 2006; Kitamura et al., 2005; Martinez et al., 2006), thereby preventing a chronic dedifferentiation process that appears to be a shared feature of otherwise different types of murine diabetes (Talchai et al., 2012b). In addition, we have recently shown that key tenets of this theory, i.e., dedifferentiation, loss of FOXO1, and conversion of β-cells into α- and δ-cells, also occur in human type 2 diabetes (Cinti et al., manuscript submitted), providing further impetus to understand how to forestall or reverse this process. This model possibly reflects an integrative function of FoxO1 downstream of heterogeneous signaling pathways, but doesn't explain the functional abnormalities that precede β-cell dedifferentiation. β-cells express also FoxO3a and 4 (Kitamura et al., 2002). The present study fills this gap in knowledge by demonstrating that, when all three FoxO isoforms are ablated, β-cells develop signal abnormalities of insulin secretion resulting in MODY-like diabetes, paving the way for eventual dedifferentiation.

Results

Rationale for the generation of triple FoxO knockout mice in β-cells

Genetic ablation of FoxO1 results in β-cell dedifferentiation following repeated pregnancies or in aging animals, as does the acquired loss of FoxO1 observed in disparate models of murine diabetes (Talchai et al., 2012b). We first investigated whether this functional loss of FoxO in diabetic islets extends to the other two isoforms, FoxO3 and FoxO4. Indeed, in islets from frankly diabetic mice (random glucose ~ 450 mg/dl), all FoxOs were decreased (Figure 1A–B). Consistent with prior data indicating that the decrease arises from hyperglycemia, and not insulin resistance (Kitamura et al., 2005), we found that high fat feeding of C57BL6 mice was insufficient to cause this abnormality (Figure S1). In FoxO1 knockout experiments, we noted a reproducible increase in the expression of FoxO3a and FoxO4 (Talchai et al., 2012b). We reasoned that this increase might mask the full phenotype due to FoxO ablation. Whereupon, we undertook to ablate the remaining two isoforms in mature β-cells, using Rip-cre mice to delete floxed *Foxo1, 3a* and *4* alleles (Paik et al.,

2007). The resulting triple knockout mice (henceforth, β-FoxO KO) were born at term in predicted Mendelian ratios, and showed no gross or growth abnormality. Using qPCR, western blotting, and immunohistochemistry, we determined that expression of the three FoxO proteins was indeed ablated (Figure 1A–C). In 12-week-old animals, islet morphology, relative content of α– and β-cells, β-cell mass, and pancreatic insulin and glucagon content were comparable between β-FoxO KO and control littermates (Figure 1D–H), as were numbers of endocrine δ– and P β-cells (data not shown). Likewise, there were no discernible differences between the two genotypes in *insulin*, *glucagon*, *somatostatin*, and *Pp* mRNA levels (Figure S1).

Early-onset, MODY-like diabetes in β-FoxO KO mice

Next, we examined *in vivo* metabolism. As early as at 12 weeks of age, β-Foxo KO mice exhibited hyperglycemia in the fasted, re-fed, and random fed states when compared to controls that included mice carrying the Rip-cre transgene, subsumed under the designation "wildtype" (see Methods) (Figure 2A). This rise was associated with lower plasma insulin levels in fasted, re-fed, and random fed animals, although the difference didn't reach statistical significance in the latter state, owing possibly to larger individual variability (Figure 2B). Likewise, we observed impaired glucose tolerance that worsened progressively with age during intraperitoneal glucose tolerance tests (Figure 2C–F), without changes to peripheral insulin sensitivity (Figure S2). The decrease in insulin levels implicated defective pancreatic endocrine function as cause of hyperglycemia.

To test insulin secretory function, we subjected mice to hyperglycemic clamps (Delghingaro-Augusto et al., 2009). After reaching steady state hyperglycemia (Figure S2), β-Foxo KO mice required a ~50% lower rate of glucose infusion to maintain it, owing to a commensurate decrease in insulin levels (Figure 2G–J). These data indicate that β-Foxo KO mice have a primary defect in glucose-dependent insulin secretion that leads to MODY-type diabetes, i.e., early-onset, mild, and moderately progressive (Fajans and Bell, 2011).

We therefore analyzed insulin secretion *in vivo* and *ex vivo*. The ability of β-FoxO KO mice to respond to the ATP-dependent K-channel blocker, glibenclamide, and to the depolarizing agent, l-arginine, was impaired (Figure 3A–B), as was the response of collagenase-purified islets challenged with varying concentrations of glucose in static incubations following overnight culture (Figure 3C). The impairment in insulin secretion occurred in very young animals, and preceded the onset of β-cell dedifferentiation (Figure S3) (Talchai et al., 2012b). Therefore, it is likely to foreshadow a more profound defect in β-cell function, possibly paving the way for dedifferentiation.

Indeed, as the animals aged to ~12 months, the previously described features of β-cell dedifferentiation emerged, as denoted by decreased expression of β-cell specific transcription factors, *Pdx1* and *MafA* and increased progenitor/pluripotency markers, *Neurogenin3* (*Ngn3*), *Nanog*, *Oct4* and *Sox2* in β-FoxO KO animals (Figure S1).

RNA profiling of FoxO-deficient islets

To understand the molecular foundation of the observed functional changes, we isolated islets from β-Foxo KO and control littermates prior to the onset of hyperglycemia in β-Foxo KO and compared transcriptomes (Table 1 and Tables S1–4). We used the Ingenuity pathway analysis to investigate alterations of known pathways and molecular interactions. Interestingly, the analysis revealed that three of the top five transcriptional networks affected by FoxO ablation were supervised by MODY genes: Hnf4αMODY 1), Hnf1α MODY3, and Pdx1 (MODY4) (Fajans and Bell, 2011) (Table 1). In addition, mitochondrial dysfunction, including ubiquinone biosynthesis (a marker of complex I activity), topped the list of canonical pathways and detoxification pathways affected by FoxO ablation (Table 1). Among listed cellular biological functions affected by triple FoxO ablation, intracellular vesicle formation, trafficking, and Ca^{2+} mobilization were predicted to have lower activities, whereas sphingolipid cleavage, oxidation of fatty acid and lipid, and transport of fatty acid were predicted to have higher activities (Table S1). Consistent with these predictions was also the activation of pathways orchestrated by nuclear receptors Pparα and Pparγ (Table S2). Interestingly, most of these alterations were also present when we analyzed transcriptomes of mice with triple FoxO knockouts in pancreatic progenitor cells, generated using Pdx1-cre mice (JY.K-M., S. Talchai, and D.A., manuscript in preparation).

Thus, the β-FoxO KO transcriptome bears significant resemblance to that of β-cells exposed to low glucose, including: decreased expression of genes involved in vesicle trafficking and Ca^{2+} mobilization, activation of Pparα and lipid oxidation (Joly et al., 2009; Roduit et al., 2000), suppression of protein synthesis, decreased cataplerosis (Flamez et al., 2002), and increased urea production (Webb et al., 2000). Interestingly, low-glucose exposure is also associated with increased oxidative stress, mimicking other aspects of the β-FoxO KO transcriptome (Tables S1–4) (Roma et al., 2012).

Metabolic inflexibility of β-FoxO KO mice

These striking findings–encompassing virtually all key pathways required for physiologic insulin secretion–allowed us to formulate a testable hypothesis on the physiologic role of the three FoxO in mature β-cells: the maintenance of physiologic insulin secretion is predicated on the cell's ability to select substrates for mitochondrial oxidative phosphorylation among glucose, lipids, and amino acids (Prentki and Madiraju, 2012), a concept known as metabolic flexibility (Figure 3D) (Galgani et al., 2008). We hypothesized that, in the absence of FoxO, β-cells lose their metabolic flexibility, and increase lipid oxidation, like starved β-cells, potentially leading to mitochondrial dysfunction through peroxide formation, generation of superoxide radicals, and impaired mitochondrial dynamics. This results in lower ATP production, reduced generation and trafficking of secretory vesicles, and decreases intracellular Ca^{2+} signaling, impairing insulin secretion (Figure 3E).

To test the metabolic flexibility of FoxO-deficient β-cells, we performed batch incubations of purified islets to measure glucose and lipid metabolism. Consistent with *in vivo* data and transcriptome analyses, we found that glucose oxidation to CO_2 was impaired by ~50% at every glucose concentration tested, except 2.8mM (Figure 4A). Glucose utilization was preserved, indicating that there is a specific defect in mitochondrial glucose metabolism

(Figure 4B) (Joly et al., 2009). Conversely, palmitate oxidation by β-FoxO KO islets in the presence of basal glucose was twofold higher, and nearly 2.5-fold higher when incubations were performed in high glucose (Figure 4C). Glycerolipid synthesis of FoxO-deficient islets, in contrast, was comparable to that of control islets at low glucose concentrations, but failed to increase at elevated glucose concentrations, resulting in lower conversion of labeled palmitate into diacylglycerides and triglycerides (Figure 4D–E). In contrast, monoacylglyceride formation was unaffected (Figure 4F), as were phospholipid and FFA synthesis (Figure S4). These data show that FoxO-deficient β-cells are impaired in their ability to switch from lipid to glucose oxidation, as glucose concentrations rise. Moreover, they show that unlike normal β-cells–which redirect acyl groups from lipid oxidation to triglyceride synthesis as glucose levels increase–FoxO-deficient β-cells appear to be locked in a lipid oxidative state. Consistent with this idea, we observed that the impairment of glucose-induced insulin release in β-FoxO KO islets could be partly reversed by adding the fatty acid oxidation inhibitor etomoxir to the culture medium. In contrast, pyruvate-induced insulin secretion was similar in islets of both genotypes (Figure S4) (Sener et al., 1978).

If metabolic inflexibility had adverse consequences on β-cell function, it should affect mitochondrial ATP generation. Hence, we tested mitochondrial function in purified islets. Basal cellular respiration (oxygen consumption rates, OCR), ATP turnover (oligomycin-sensitive respiration), proton leak (oligomycin-insensitive respiration), and maximal respiration (FCCP-induced) were identical between control and knockout animals. Raising glucose concentrations from 3 to 20mM more than doubled ATP turnover in control islets, but had hardly any effect in KO islets. Addition of the electron transport chain inhibitor rotenone suppressed OCR in both groups to the same extent, indicating that non-mitochondrial respiration was unaffected (Figure 5A). As a result of the decreased glucose-induced oxygen consumption, the glucose-dependent OCR area under the curve was reduced by 35% in β-FoxO KO islets (Figure 5B). The selective impairment of glucose-dependent OCR is consistent with RNA profiling data of lower complex I function.

Insulin secretion is induced by rising ATP/ADP ratios (Matschinsky, 1996). The ADP-stimulated rate, calculated as the difference between coupled OCR and basal OCR, was >60% lower in β-FoxO KO islets (Figure 5C). Finally, glucose-induced ATP generation was also blunted in β-FoxO KO (Figure 5D). These changes were not related to changes in mitochondria size and density as assessed by electron microscopy (data not shown). The mitochondrial analysis thus supports the hypothesis of impaired metabolic flexibility.

Ca^{2+} mobilization is required for proper intracellular assembly and mobilization of secretory vesicles, leading to insulin exocytosis (Rorsman et al., 2012). mRNA profiling data were consistent with impaired activation of networks required for Ca^{2+} mobilization, signaling, and vesicle transport in β-FoxO KO mice (Table S1). Accordingly, we found that membrane depolarization-induced Ca^{2+} influx in response to rising glucose concentrations was considerably lower in β-cells lacking FoxO (Figure 6A). β–FoxO KO islets showed lower levels of mRNAs encoding α-subunits of L-type voltage-gated Ca^{2+} channels, Ca^{2+}-dependent as well as Ca^{2+}-independent (but PMA sensitive) protein kinase C, inositol-phosphate receptors 1–3, and several phospholipase C isoforms (Figure 6B). We also validated RNA profiling data by measuring expression of a subset of target genes in calcium

metabolism (Figure S5). To provide functional evidence for these changes, we examined insulin secretion from purified islets in response to a variety of Ca^{2+}-dependent secretagogues. We found lower insulin secretion in response to the sulfonylurea glibenclamide, the PKC activator PMA, and the L-type Ca channel activator Bay-K8644. In contrast, responses to the cAMP-agonists IBMX and forskolin were preserved (Figure 6C).

Discussion

The key finding of this work is that a complete loss FoxO function that includes FoxO1, 3a, and 4–as might be expected in multiple forms of β-cell dysfunction (Talchai et al., 2012b)–causes MODY-like diabetes through reduced metabolic flexibility of β-cells. Our interpretation is that FoxOs are collectively required to maintain MODY-related gene networks, which in turn are required to enable a gene expression program that permits proper substrate selection (glucose *vs*. fatty acids) for mitochondrial oxidative phosphorylation. We suggest that metabolic inflexibility caused by progressive loss of FoxO (Talchai et al., 2012b) is the mechanism underlying the progression from impaired insulin secretion to dedifferentiation, leading to a loss of β-cell mass.

FoxOs are activated by hyperglycemia-induced oxidative stress in β-cells (Kawamori et al., 2006; Kitamura et al., 2005). Under appropriate experimental conditions, there is a transient effect of glucose to promote FoxO nuclear exclusion, arguably in response to autocrine insulin signaling (Martinez et al., 2006). But this may reflect a specific situation made possible by the lower insulin content and more extreme glucose deprivation in vitro, rather than a physiologic mechanisms, as we have suggested (Kitamura et al., 2005). We have proposed that, as they rapidly respond to the β-cell's nutritional state, FoxO are better positioned to translate the latter into an appropriate transcriptional programa than other transcription factors that don't respond as nimbly to changes in glucose, lipid, and hormone levels. (Talchai et al., 2009) If the stress persists, FoxO levels drop through deacetylation-induced degradation that prevents the normal autoregulatory loop of FoxO expression (Kitamura et al., 2005; Talchai et al., 2012a). We now report that the loss of all three FoxO (likely through similar mechanisms) impairs the homeostatic MODY-related gene network, and activates Pparα-dependent lipid oxidative pathways, possibly resulting in increased supply of fatty acyl-derived acetyl-CoA for mitochondrial oxidation. That β-FoxO KO islets fail to support glucose-induced diacylglycerol and TG synthesis despite the predicted activation of the Pparγ network, suggests that the latter event has a compensatory character, possibly aimed at preventing excessive lipid oxidation. This finding provides a potential explanation for the clinical benefits of Pparγ agonists on β-cell function, i.e., that they shunt lipids from oxidation to synthesis, preventing lipid-fueled toxicity (Defronzo et al., 2013; Leahy, 2009). Enhanced fatty acid oxidation and reduced lipid esterification processes will also result in altered glycerolipid/fatty acid cycling and production of lipid mediators for glucose-induced insulin secretion (Prentki et al., 2013). Thus, FoxO appear to control both mitochondrial (e.g., ATP) and lipid signals for glucose-stimulated insulin release.

How do FoxO oversee such a vast functional β-cell network? A potential explanation is that FoxO are required to enforce the HNF4α network, and that the others are dependent on HNF4α (Gupta et al., 2005; Odom et al., 2004)Alternatively, FoxO could be orchestrating

higher-level changes in genome maintenance, for example through Hic1, a transcriptional repressor with a potential role in genome methylation (Pinte et al., 2004) that figures prominently among FoxO transcriptome changes, and regulates two important networks in β-cell function, Tcf7L2 and EphA2. (Foveau et al., 2012; Valenta et al., 2006)

When viewed in the context of prior data indicating a role of FoxO in the acute response to hyperglycemia-induced oxidative stress (Kawamori et al., 2006; Kitamura et al., 2005), and the chronic role of FoxO1 in β-cell lineage maintenance and differentiation (Talchai et al., 2012b), the data begin to outline a unified theory that bridges the two cornerstones of diabetic β-cell failure: reduced function and impaired mass (Accili et al., 2010). Not only that, but the data provide a heretofore missing link between metabolic alterations and regulation of MODY1, 3, and 4 genes that serves as a paradigm for the connection between genetic and acquired β-cell abnormalities. The transcriptome of FoxO-deficient β-cells provides a rich menu to design better therapies to combat β-cell dysfunction in type 2 diabetes.

Methods

Animals

We performed genotyping as described (Kitamura et al., 2009; Tsuchiya et al., 2012). Mice were maintained on a mixed 129J-C57BL/6 background. As controls, owing to the complexity of genotyping the 6 mutant alleles (five Foxo alleles and Rip-cre), we used different combinations of FoxO1, 3 and 4 floxed mice without Rip-cre transgene or Rip-cre mice without FoxO floxed alleles (Xuan et al., 2002). These mice were indistinguishable from mixed 129J-C57BL/6 mice in all metabolic tests. All mice were fed normal chow and maintained on a 12–hour light–dark cycle (lights on at 7 AM). All experiments were performed in 12- to 20-week-old male mice, unless specified otherwise in figure legends. The Columbia University Institutional Animal Care and Utilization Committee approved all experiments.

RNA profiling

We used GeneChip Mouse Exon arrays (Affymetrix) and performed data analysis with Partek Genomics Suite (Partek, Inc.) and Ingenuity Pathway Analysis (Ingenuity System, Inc.). For the analyses shown in this study, we used a threshold of $p < 0.05$ and >1.3-fold change ($n = 4$ WT, 3 KO per group. Each array was performed with pooled islets from 3 mice per genotype.).

Metabolic analyses

We performed glucose tolerance tests in overnight-fasted mice by intraperitoneal injection of glucose (2 g/kg) (Xuan et al., 2010). We performed GSIS and arginine-induced insulin secretion tests as described (Kido et al., 2000). We measured glucagon by radioimmunoassay and insulin by ELISA (Millipore). We performed hyperglycemic glucose clamps as described (Delghingaro-Augusto et al., 2009).

Immunoblot, immunohistochemistry and morphometry

Western blots used the primary antibodies directed against the following proteins: Foxo1, Foxo3, Foxo4, α-tubulin from Cell Signaling (#2880, 2497, 9472, and 2144). We fixed and processed tissues for immunohistochemistry as described (Kitamura et al., 2009). We applied perfused fixation, and antigen retrieval for nuclear transcription factor detection (Nacalai USA) (Talchai et al., 2012b). We used anti-Foxo1 (Cell Signaling #2880), anti-insulin and anti-glucagon from Dako (#A056401-2, A056501-2) for primary antibodies and FITC-, Cy3-, and Alexa-conjugated donkey secondary antibodies (Jackson Immunoresearch Laboratories, and Molecular Probes)(Kitamura et al., 2009). Antibodies to Pcsk1, Pcsk2, Glut-2 and Pdx-1 were from EMD Millipore (#AB10553, AB15610, 07-1402, 061384). For β-cell morphometry, 4 pancreatic sections from 4 mice from each genotype were sampled 150 μm apart, and used for a two-tailed paired Student's t-test analysis. Total pancreas area was captured at 100x, and immunostaining area at 200x (Talchai et al., 2012b). The ratio of immunoreactive area/pancreas area was converted from pixel to mm^2 and plotted as mm^2.

Mitochondrial function

We used the XF24-3 respirometer (Seahorse Bioscience) with 24-well plates designed to confine islets. We used the F_1F_0 ATP synthase inhibitor oligomycin to assess uncoupling, FCCP to estimate maximum respiration, and rotenone to measure non-mitochondrial respiration (Qiang et al., 2012).

Ca^{2+} influx

We isolated pancreatic islets by collagenase digestion and resuspended them in RPMI. Fura-2 fluorescence was recorded (Delta Ram; PTI Inc., South Brunswick, NJ) in an RC-20 bath flow chamber (Warner Instrument Corp., Hamden, CT), at excitation wavelengths of 340 and 380 nm (Srivastava et al., 2012). Data are represented as 340/380 ratios after background subtraction.

Glucose and lipid metabolism

After overnight recovery and 2-hr starvation, 20 islets were pre-incubated in KRBH for 45min at 2.8mM glucose followed by incubation in KRBH containing 0.5 μCi of [5-^{3}H] D-glucose (16 Ci/mmol) and 1μCi/ml [U-^{14}C] D-glucose (250 mCi/mmol) at 2.8, 8.3 and 16.7mM glucose. Incubation was terminated by the addition of citrate/NaOH buffer (400 mM, pH 4.9) containing antimycin-A (10 M), rotenone (10 M), and KCN (5 mM). Glucose oxidation was measured by the generation of KO- trapped $^{14}CO_2$ after 60-min (Buteau et al., 2007). Glucose utilization was determined by measuring ^3H_2O (Buteau et al., 2007). Lipid oxidation and triglyceride synthesis from glycerol were measured as described (Delghingaro-Augusto et al., 2009). Islets were cultured in RPMI with 5.5 mM glucose, 0.25% (w/v) defatted BSA, 0.1 mM palmitate and [9,10(n)-^{3}H]-palmitate (74 kBq/ml) for 16 hr at 37°C. They were washed in KRBH supplemented with 0.25% (w/v) BSA, 3 mM glucose and 0.1 mM palmitate, followed by 2-hr incubation in KRBH supplemented with 0.25% (w/v) BSA, 0.1 mM palmitate, [9,10(n)-^{3}H]-palmitate (74 kBq/ml), 1 mM carnitine, and 3, 8, or 16 mM glucose. The supernatant was collected and frozen to separate ^3H_2O from labeled fatty acids prior to counting ^3H_2O radioactivity. For fatty acid esterification,

islets were cultured for 16 hr at 37°C in RPMI with 3 or 16 mM glucose, 0.25% (w/v) defatted BSA, 0.1 mM palmitate and [1-^{14}C]-palmitate (37 kBq/ml). They were collected, washed and resuspended in Folch reagent. Total lipids were extracted and separated by thin-layer chromatography using petroleum ether/ethyl–ether/acetic acid (70:30:1). Spots corresponding to phospholipids, monoacylglycerol, diacylglycerol and triacylglycerol were visualized by autoradiography, and counted (Delghingaro-Augusto et al., 2009).

RNA measurements

We used standard techniques for mRNA isolation and quantitative PCR. PCR primer sequences have been published (Talchai et al., 2012b).

Statistical analyses and general methods

Sample sizes were estimated from expected effect size based on previous experiments. No randomization or blinding was used. We present data as means ± SEM. We used two-tailed Student's t-test, one-way ANOVA, or two-way ANOVA for data analysis, and the customary threshold of $p < 0.05$ to declare statistically significant differences.

Supplementary Material

Refer to Web version on PubMed Central for supplementary material.

Acknowledgments

Supported by grants from NIH DK64819, DK63608 (Columbia University Diabetes Research Center), DK20541 (Einstein College of Medicine Diabetes Research Center), Brehm Coalition, JPB Foundation, Canadian Institute of Health Research, Diabète Québec, Montreal Diabetes Research Center, and Fonds de Recherche du Québec Santé. MP holds the Canada Chair in diabetes and metabolism. We are grateful to members of the Accili laboratory for insightful data discussions. We thank Mr. Thomas Kolar and Ms. Ana Flete-Castro (Columbia University) for outstanding technical support.

References

Accili D, Ahren B, Boitard C, Cerasi E, Henquin JC, Seino S. What ails the beta-cell? Diabetes Obes Metab. 2010; 12(Suppl 2):1–3. [PubMed: 21029293]

Buteau J, Shlien A, Foisy S, Accili D. Metabolic diapause in pancreatic beta-cells expressing a gain-of-function mutant of the forkhead protein Foxo1. The Journal of biological chemistry. 2007; 282:287–293. [PubMed: 17107961]

Defronzo RA, Tripathy D, Schwenke DC, Banerji M, Bray GA, Buchanan TA, Clement SC, Gastaldelli A, Henry RR, Kitabchi AE, et al. Prevention of Diabetes with Pioglitazone in Act Now: Physiologic Correlates. Diabetes. 2013

Delghingaro-Augusto V, Nolan CJ, Gupta D, Jetton TL, Latour MG, Peshavaria M, Madiraju SR, Joly E, Peyot ML, Prentki M, et al. Islet beta cell failure in the 60% pancreatectomised obese hyperlipidaemic Zucker fatty rat: severe dysfunction with altered glycerolipid metabolism without steatosis or a falling beta cell mass. Diabetologia. 2009; 52:1122–1132. [PubMed: 19294363]

Fajans SS, Bell GI. MODY: history, genetics, pathophysiology, and clinical decision making. Diabetes Care. 2011; 34:1878–1884. [PubMed: 21788644]

Ferrannini E. The stunned beta cell: a brief history. Cell metabolism. 2010; 11:349–352. [PubMed: 20444416]

Flamez D, Berger V, Kruhoffer M, Orntoft T, Pipeleers D, Schuit FC. Critical role for cataplerosis via citrate in glucose-regulated insulin release. Diabetes. 2002; 51:2018–2024. [PubMed: 12086928]

Foveau B, Boulay G, Pinte S, Van Rechem C, Rood BR, Leprince D. The receptor tyrosine kinase EphA2 is a direct target gene of hypermethylated in cancer 1 (HIC1). J Biol Chem. 2012; 287:5366–5378. [PubMed: 22184117]

Galgani JE, Moro C, Ravussin E. Metabolic flexibility and insulin resistance. Am J Physiol Endocrinol Metab. 2008; 295:E1009–1017. [PubMed: 18765680]

Gupta RK, Vatamaniuk MZ, Lee CS, Flaschen RC, Fulmer JT, Matschinsky FM, Duncan SA, Kaestner KH. The MODY1 gene HNF-4alpha regulates selected genes involved in insulin secretion. J Clin Invest. 2005; 115:1006–1015. [PubMed: 15761495]

Joly E, Roduit R, Peyot ML, Habinowski SA, Ruderman NB, Witters LA, Prentki M. Glucose represses PPARalpha gene expression via AMP-activated protein kinase but not via p38 mitogen-activated protein kinase in the pancreatic beta-cell. Journal of diabetes. 2009; 1:263–272. [PubMed: 20923527]

Kawamori D, Kaneto H, Nakatani Y, Matsuoka TA, Matsuhisa M, Hori M, Yamasaki Y. The forkhead transcription factor Foxo1 bridges the JNK pathway and the transcription factor PDX-1 through its intracellular translocation. J Biol Chem. 2006; 281:1091–1098. [PubMed: 16282329]

Kido Y, Burks DJ, Withers D, Bruning JC, Kahn CR, White MF, Accili D. Tissue-specific insulin resistance in mice with mutations in the insulin receptor, IRS-1, and IRS-2. The Journal of clinical investigation. 2000; 105:199–205. [PubMed: 10642598]

Kitamura T, Kitamura YI, Kobayashi M, Kikuchi O, Sasaki T, Depinho RA, Accili D. Regulation of pancreatic juxtaductal endocrine cell formation by FoxO1. Molecular and cellular biology. 2009; 29:4417–4430. [PubMed: 19506018]

Kitamura T, Nakae J, Kitamura Y, Kido Y, Biggs WH 3rd, Wright CV, White MF, Arden KC, Accili D. The forkhead transcription factor Foxo1 links insulin signaling to Pdx1 regulation of pancreatic beta cell growth. The Journal of clinical investigation. 2002; 110:1839–1847. [PubMed: 12488434]

Kitamura YI, Kitamura T, Kruse JP, Raum JC, Stein R, Gu W, Accili D. FoxO1 protects against pancreatic beta cell failure through NeuroD and MafA induction. Cell metabolism. 2005; 2:153–163. [PubMed: 16154098]

Leahy JL. Thiazolidinediones in prediabetes and early type 2 diabetes: what can be learned about that disease's pathogenesis. Current diabetes reports. 2009; 9:215–220. [PubMed: 19490823]

Martinez SC, Cras-Meneur C, Bernal-Mizrachi E, Permutt MA. Glucose Regulates Foxo1 Through Insulin Receptor Signaling in the Pancreatic Islet {beta}-cell. Diabetes. 2006; 55:1581–1591. [PubMed: 16731820]

Matschinsky FM. Banting Lecture 1995. A lesson in metabolic regulation inspired by the glucokinase glucose sensor paradigm. Diabetes. 1996; 45:223–241. [PubMed: 8549869]

Matsumoto M, Han S, Kitamura T, Accili D. Dual role of transcription factor FoxO1 in controlling hepatic insulin sensitivity and lipid metabolism. The Journal of clinical investigation. 2006; 116:2464–2472. [PubMed: 16906224]

Nakae J, Kitamura T, Kitamura Y, Biggs WH 3rd, Arden KC, Accili D. The forkhead transcription factor Foxo1 regulates adipocyte differentiation. Developmental cell. 2003; 4:119–129. [PubMed: 12530968]

National Institute of Diabetes and Digestive and Kidney Diseases. National Diabetes Statistics fact sheet: general information and national estimates on diabetes in the United States. Bethesda, MD: U.S. Department of Health and Human Services, National Institute of Health; 2005.

Odom DT, Zizlsperger N, Gordon DB, Bell GW, Rinaldi NJ, Murray HL, Volkert TL, Schreiber J, Rolfe PA, Gifford DK, et al. Control of pancreas and liver gene expression by HNF transcription factors. Science. 2004; 303:1378–1381. [PubMed: 14988562]

Paik JH, Kollipara R, Chu G, Ji H, Xiao Y, Ding Z, Miao L, Tothova Z, Horner JW, Carrasco DR, et al. FoxOs Are Lineage-Restricted Redundant Tumor Suppressors and Regulate Endothelial Cell Homeostasis. Cell. 2007; 128:309–323. [PubMed: 17254969]

Pinte S, Stankovic-Valentin N, Deltour S, Rood BR, Guerardel C, Leprince D. The tumor suppressor gene HIC1 (hypermethylated in cancer 1) is a sequence-specific transcriptional repressor: definition of its consensus binding sequence and analysis of its DNA binding and repressive properties. J Biol Chem. 2004; 279:38313–38324. [PubMed: 15231840]

Prentki M, Madiraju SR. Glycerolipid/free fatty acid cycle and islet beta-cell function in health, obesity and diabetes. Mol Cell Endocrinol. 2012; 353:88–100. [PubMed: 22108437]

Prentki M, Matschinsky FM, Madiraju SR. Metabolic signaling in fuel-induced insulin secretion. Cell Metab. 2013; 18:162–185. [PubMed: 23791483]

Qiang L, Wang L, Kon N, Zhao W, Lee S, Zhang Y, Rosenbaum M, Zhao Y, Gu W, Farmer SR, et al. Brown Remodeling of White Adipose Tissue by SirT1-Dependent Deacetylation of Ppargamma. Cell. 2012; 150:620–632. [PubMed: 22863012]

Rahier J, Guiot Y, Goebbels RM, Sempoux C, Henquin JC. Pancreatic beta-cell mass in European subjects with type 2 diabetes. Diabetes Obes Metab. 2008; 10(Suppl 4):32–42. [PubMed: 18834431]

Reaven GM. Pathophysiology of insulin resistance in human disease. Physiol Rev. 1995; 75:473–486. [PubMed: 7624391]

Roduit R, Morin J, Masse F, Segall L, Roche E, Newgard CB, Assimacopoulos-Jeannet F, Prentki M. Glucose down-regulates the expression of the peroxisome proliferator-activated receptor-alpha gene in the pancreatic beta -cell. J Biol Chem. 2000; 275:35799–35806. [PubMed: 10967113]

Roma LP, Pascal SM, Duprez J, Jonas JC. Mitochondrial oxidative stress contributes differently to rat pancreatic islet cell apoptosis and insulin secretory defects after prolonged culture in a low non-stimulating glucose concentration. Diabetologia. 2012; 55:2226–2237. [PubMed: 22643931]

Rorsman P, Braun M, Zhang Q. Regulation of calcium in pancreatic alpha- and beta-cells in health and disease. Cell calcium. 2012; 51:300–308. [PubMed: 22177710]

Savage PJ, Bennion LJ, Flock EV, Nagulesparan M, Mott D, Roth J, Unger RH, Bennett PH. Diet-induced improvement of abnormalities in insulin and glucagon secretion and in insulin receptor binding in diabetes mellitus. J Clin Endocrinol Metab. 1979; 48:999–1007. [PubMed: 447806]

Sener A, Kawazu S, Hutton JC, Boschero AC, Devis G, Somers G, Herchuelz A, Malaisse WJ. The stimulus-secretion coupling of glucose-induced insulin release. Effect of exogenous pyruvate on islet function. Biochem J. 1978; 176:217–232. [PubMed: 365174]

Srivastava S, Cai X, Li Z, Sun Y, Skolnik EY. Phosphatidylinositol-3-kinase C2beta and TRIM27 function to positively and negatively regulate IgE receptor activation of mast cells. Mol Cell Biol. 2012; 32:3132–3139. [PubMed: 22645315]

Talchai C, Lin HV, Kitamura T, Accili D. Genetic and biochemical pathways of beta-cell failure in type 2 diabetes. Diabetes Obes Metab. 2009; 11(Suppl 4):38–45. [PubMed: 19817787]

Talchai C, Xuan S, Kitamura T, Depinho RA, Accili D. Generation of functional insulin-producing cells in the gut by Foxo1 ablation. Nat Genet. 2012a; 44:406–412. [PubMed: 22406641]

Talchai C, Xuan S, Lin HV, Sussel L, Accili D. Pancreatic beta Cell Dedifferentiation as a Mechanism of Diabetic beta Cell Failure. Cell. 2012b; 150:1223–1234. [PubMed: 22980982]

Tsuchiya K, Tanaka J, Shuiqing Y, Welch CL, Depinho RA, Tabas I, Tall AR, Goldberg IJ, Accili D. FoxOs Integrate Pleiotropic Actions of Insulin in Vascular Endothelium to Protect Mice from Atherosclerosis. Cell metabolism. 2012; 15:372–381. [PubMed: 22405072]

Valenta T, Lukas J, Doubravska L, Fafilek B, Korinek V. HIC1 attenuates Wnt signaling by recruitment of TCF-4 and beta-catenin to the nuclear bodies. Embo J. 2006; 25:2326–2337. [PubMed: 16724116]

Webb GC, Akbar MS, Zhao C, Steiner DF. Expression profiling of pancreatic beta cells: Glucose regulation of secretory and metabolic pathway genes. Proc Natl Acad Sci U S A. 2000; 97:5773–5778. [PubMed: 10811900]

Weyer C, Bogardus C, Mott DM, Pratley RE. The natural history of insulin secretory dysfunction and insulin resistance in the pathogenesis of type 2 diabetes mellitus. J Clin Invest. 1999; 104:787–794. [PubMed: 10491414]

Xuan S, Kitamura T, Nakae J, Politi K, Kido Y, Fisher PE, Morroni M, Cinti S, White MF, Herrera PL, et al. Defective insulin secretion in pancreatic beta cells lacking type 1 IGF receptor. The Journal of clinical investigation. 2002; 110:1011–1019. [PubMed: 12370279]

Xuan S, Szabolcs M, Cinti F, Perincheri S, Accili D, Efstratiadis A. Genetic analysis of type-1 insulin-like growth factor receptor signaling through insulin receptor substrate-1 and -2 in pancreatic beta cells. The Journal of biological chemistry. 2010; 285:41044–41050. [PubMed: 20947509]

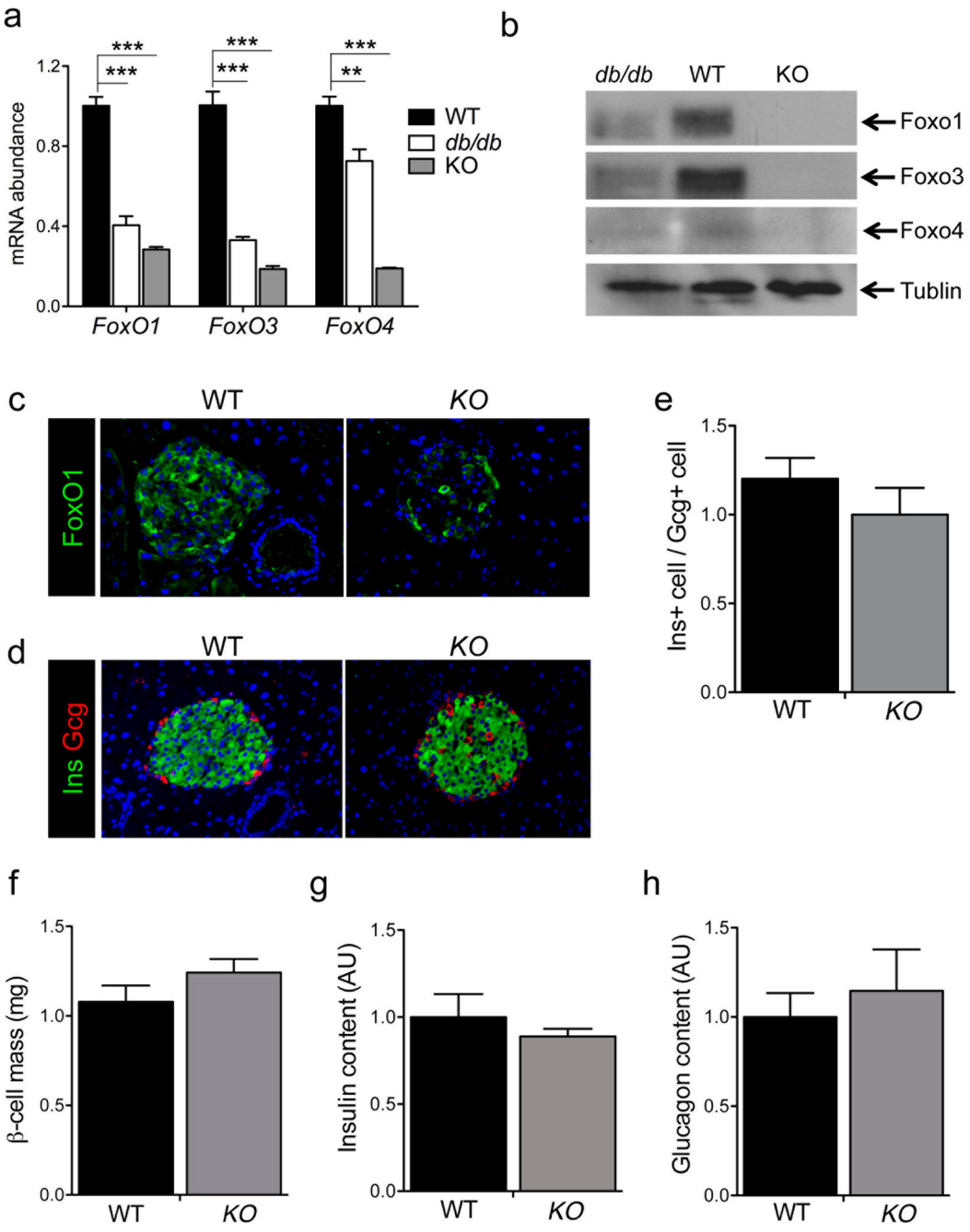

Figure 1. Expression of FoxO in diabetic islets and generation of triple FoxO knockouts in β-cells

(A–B) mRNA levels (arbitrary units, AU) and Western blot analysis of the three FoxO isoforms in islet extracts of 24-week-old *db/db*, WT (*C57BL/6*) and KO (each islet extract was prepared with pooled islets from 2–3 mice per genotype).

(C–D) Representative islet immunohistochemistry using antibodies against FoxO1 (c, green), insulin (Ins, green in D), or glucagon (Gcg, red in D). Nucleus is stained blue with DAPI.

(E) Ratio of insulin- to glucagon-immunoreactive areas as determined by immunohistochemistry (n=4 mice per genotype, 6 sections per mouse).
(F) Morphometric analysis of β-cell mass in 12-week-old mice (n=4 mice per genotype, 4 sections per mouse).
(G–H) Quantification of insulin and glucagon content in acid-ethanol extracts from collagenase-purified islets (n=5 mice per group). All data are presented as means ± SEM. $^{**}p<0.01$, $^{***}p<0.001$ by Student's *t* test.

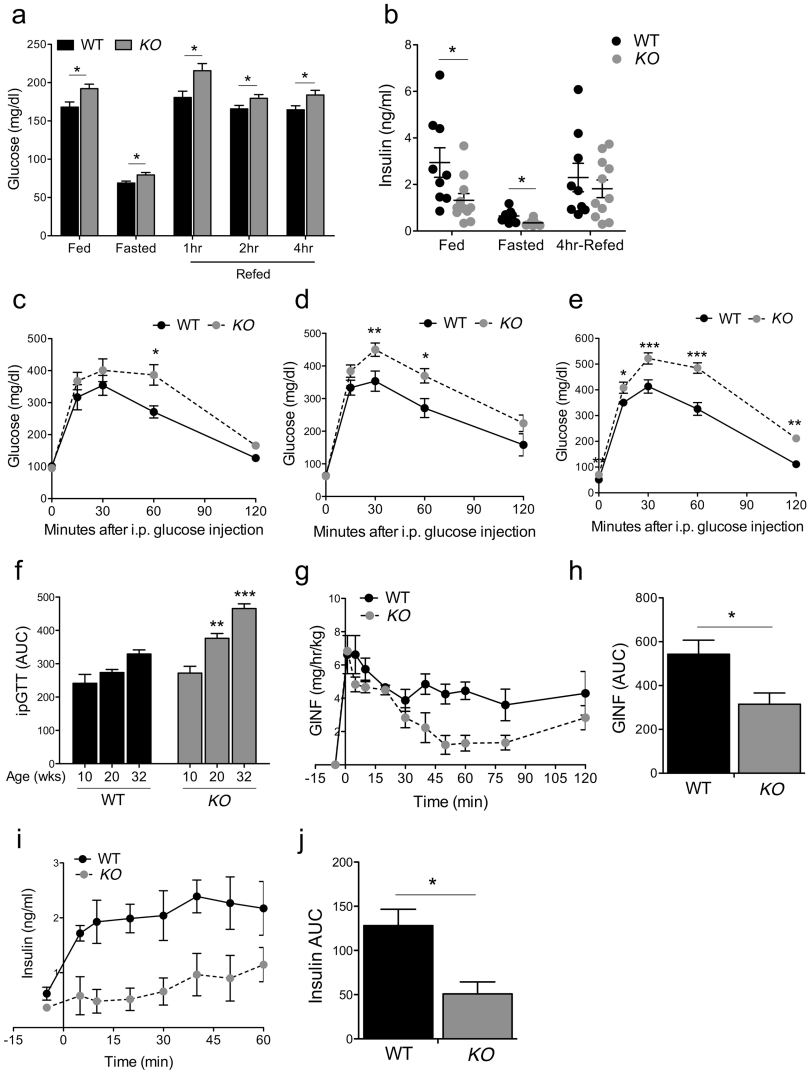

Figure 2. Metabolic analyses in β-FoxO KO mice

(A–B) Blood glucose and insulin levels in fasted, fed, and 4-hr-refed 12-week-old male mice (n=9 WT, 10 KO mice per genotype).

(C–E) Intraperitoneal glucose tolerance tests in male mice at different ages (n=12 WT, 8 KO mice per genotype at each age).

(F) Quantification of areas under the curve for the experiments shown in c-e.

(G–I) Hyperglycemic clamps in 24-week-old male mice, showing glucose infusion rates (G), plasma insulin levels (I) and quantification of areas under the curve for the experiments shown in h and i (n=4 mice per genotype). All data are presented as means ± SEM. *p<0.05, **p<0.01, ***p<0.001 by two-way ANOVA.

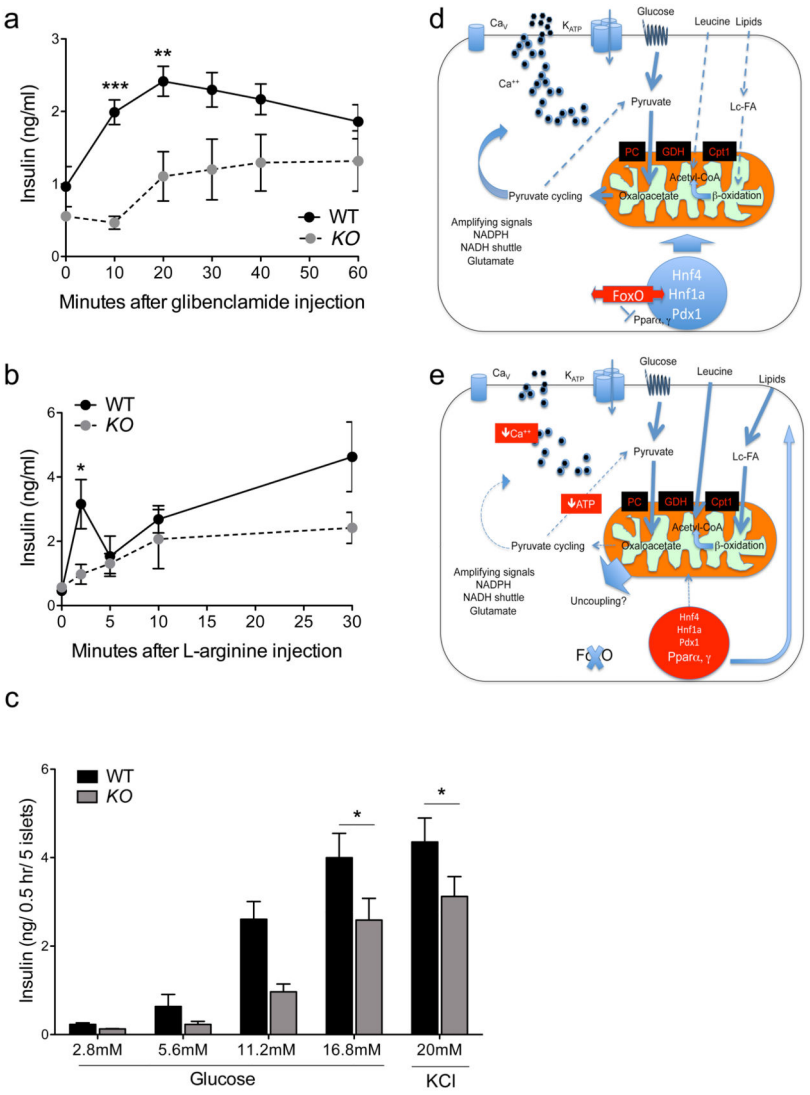

Figure 3. Insulin secretion and working model

(A–B) Glibenclamide- and l-arginine-induced insulin secretion *in vivo* (n=8 mice per group). (C) Glucose-induced insulin release from collagenase-purified islets stimulated with glucose or KCl (n=3 per group). Each experiment was performed with pooled islets from 3–4 mice per genotype. Each data point consists of 4 replicates. All data are presented as means ± SEM. **p*<0.05, ***p*<0.01, ****p*<0.001 by two-way ANOVA (A–B) or one-factor ANOVA (C).

(D–E) Model of FoxO regulation of insulin secretion in pathophysiologic conditions. FoxO nuclear translocation mediates the effects of glucose on gene expression through MODY gene networks (Buteau et al., 2007; Kitamura et al., 2005), allowing glucose flux into mitochondria (thick arrows), with smaller contributions by lipids and amino acids (thin dotted arrows). (E) As FoxO become functionally exhausted, β-cells are transcriptionally blindsided to the effects of glucose, increasing lipid and amino acid flux. MODY genes are suppressed, and Ppar's increased, consistent with the role of FoxO to suppress Pparα in liver

(Matsumoto et al., 2006) and Pparγ in fat (Nakae et al., 2003). PC: Pyruvate carboxylase; GDH: glutamate dehydrogenase; Cpt1: carnitine palmitoyltransferase-1.

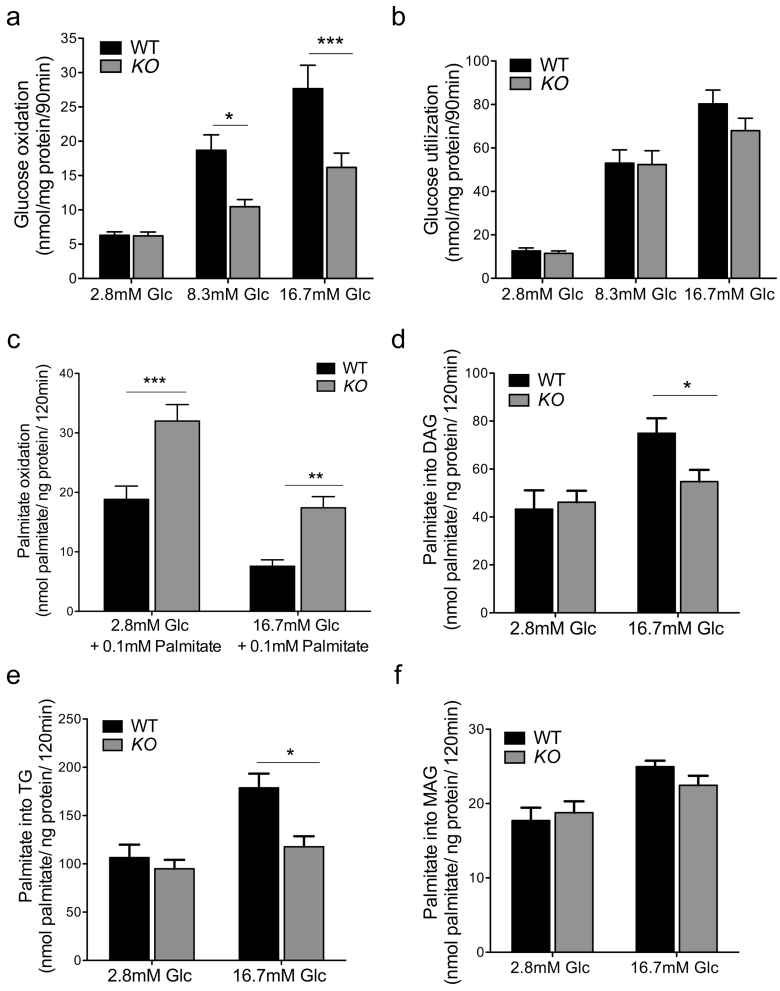

Figure 4. Glucose and lipid metabolism in isolated islets

(A) ^{3}H-glucose oxidation,

(B) ^{14}C-glucose utilization,

(C) palmitate oxidation,

(D–F) diacylglycerol (D), triglyceride (E), and monoacylglycerol synthesis (F) from ^{14}C-labeled palmitate (n=3 per group). Each experiment was performed with pooled islets from 5 mice per genotype. Each data point consists of 6–9 replicates. Glc: glucose, Pal: palmitate. All data are presented as means ± SEM. *p<0.05, **p<0.01, ***p<0.001 by Student's t test.

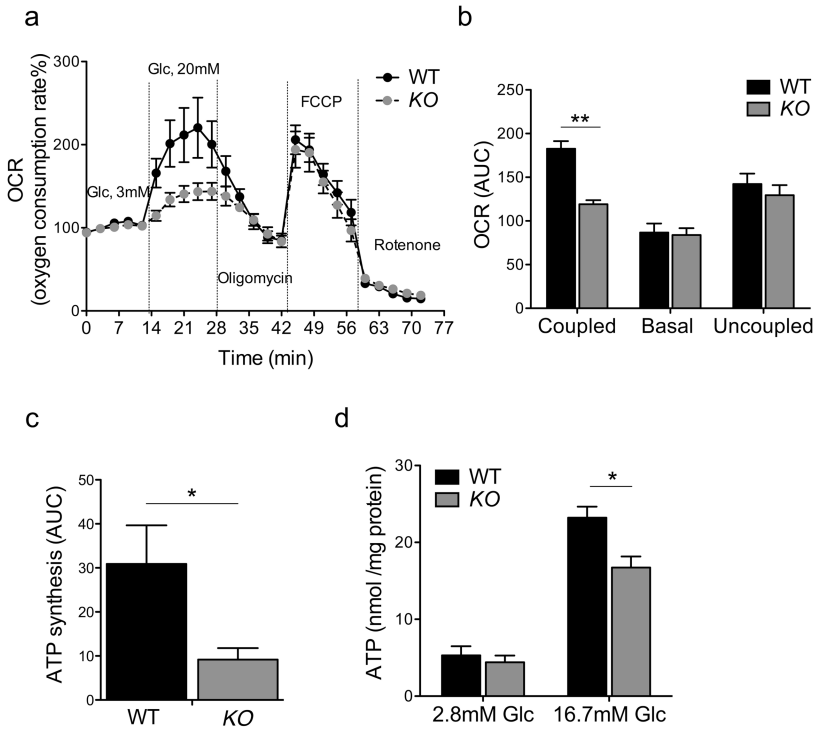

Figure 5. Mitochondrial function in isolated islets

(A–B) Time course and area under the curve (AUC) of oxygen consumption rates measured in collagenase-purified islets from wildtype and β-FoxO KO mice. Oligomycin inhibits ATP synthase, FCCP is an uncoupler, and rotenone an inhibitor of complex I (n=3 per group). Each experiment was performed with pooled islets from 5 mice per genotype. Each data point consists of 10 replicates.

(C) ADP-stimulated rate of ATP generation, calculated as the difference between coupled and basal OCR.

(D) ATP content of pancreatic islets of wildtype and β-FoxO mice quantified at different glucose concentrations (n=3 per group). Each experiment was performed with pooled islets from 3 mice per genotype. Each data point consists of 5 replicates. All data are presented as means ± SEM. *p<0.05, **p<0.01 by Student's t test.

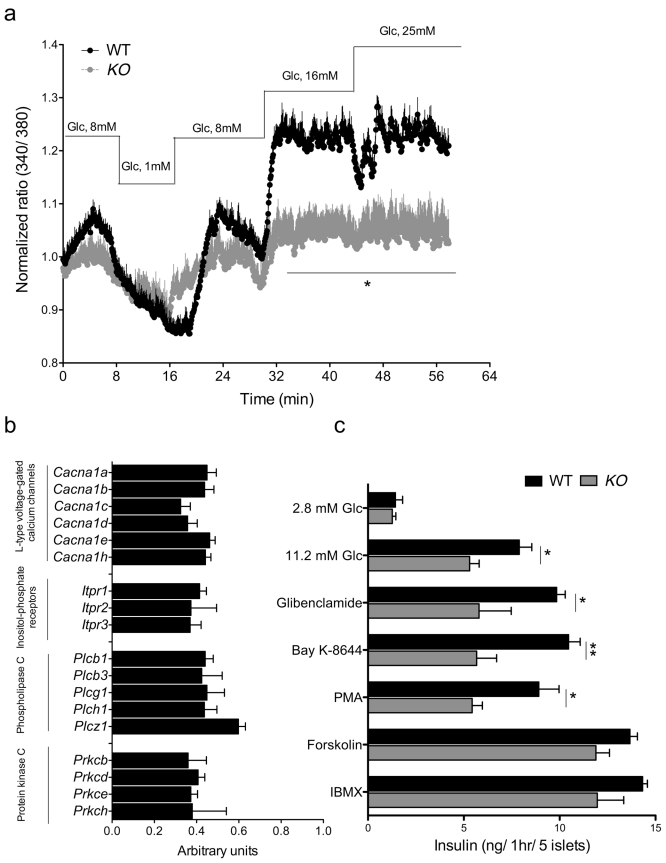

Figure 6. Ca^{2+} flux in isolated islets

(A) Ca^{2+} influx measured by Fura2 AM loading in isolated islets incubated with the indicated amounts of glucose (n=3 per group). Each experiment was performed with pooled islets from 2 mice per genotype. Each data point consists of 4 replicates. All data are presented as means ± SEM. * p <0.05 by one-factor ANOVA.

(B) mRNA levels of genes involved in Ca homeostasis, *Cacna*: α-subunits isoforms of L-type voltage-gated Ca^{2+} channels; Itpr: inositolphosphate receptor; *Pkc*: Ca^{2+}-sensitive and -insensitive protein kinase C; *Plc*: phospholipase C. Data are expressed as percent of wildtype values and were obtained in pancreatic islets of 10-week-old control and β-FoxO mice (n=9–12 per genotype).

(C) Secretagogue-stimulated insulin secretion in isolated islets incubated with glucose (2.8mM and 11.2mM), glibenclamide (1μM), PMA (1μM), Bay K-8644 (0.5μM), forskolin (5μM), IBMX (0.5mM) in the presence of 11.2mM glucose (n=3 per group). Each experiment was performed with pooled islets from 5 mice per genotype. Each data point consists of 4 replicates. PMA: *Phorbol myristate acetate; IBMX:* 3-isobutyl-1-methylxanthine. All data are presented as means ± SEM. *p<0.05, **p<0.01 by Student's t test.

Table 1

Summary of pathway analysis of transcriptome data

Pathway	Top genes	p value
Transcription regulator	Hnf4α	2.0×10^{-14}
	Hic1	1.8×10^{-3}
	Hnf1α	1.8×10^{-3}
	Nfe2L2	5.0×10^{-3}
	Pdx1	6.2×10^{-3}
Canonical pathways	Mitochondrial dysfunction	5.9×10^{-7}
	Ubiquinone biosynthesis	8.0×10^{-6}
	Purine metabolism	8.8×10^{-5}
	Lysine degradation	1.5×10^{-4}
	Valine, Leucine and Isoleucine Degradation	7.7×10^{-4}
"Toxic" list	Mitochondrial dysfunction	1.0×10^{-6}
	Glutathione depletion	2.9×10^{-2}
	Fatty acid metabolism	5.0×10^{-2}
	LXR/RXR activation	8.0×10^{-2}
	Oxidative stress	1.0×10^{-1}
Biological functions	Energy production	1.5×10^{-4} to 3×10^{-2}
	Molecular transport	1.5×10^{-4} to 3.4×10^{-2}
	Nucleic acid metabolism	1.5×10^{-4} to 3.4×10^{-2}
	Small molecule biochemistry	1.5×10^{-4} to 4.2×10^{-2}
	Cellular assembly and organization	1.7×10^{-4} to 4.2×10^{-2}

The table summarizes top pathways and transcription factors from transcriptome analysis of β-FoxO KO mice.